ASEISMIC CHARACTERISTICS OF RC BOX AND CYLINDER WALLS

by

Hajime Umemura,[I] Hiroyuki Aoyama,[II] Masaru Ito[III]
and Youji Hosokawa[IV]

SYNOPSIS

This study was conducted to investigate the behavior of box and cylinder type shear walls under cyclic loading simulating earthquake forces on walls of atomic reactors and other structures. Seven specimens, five box type and two cylinder type, were tested. Initial stiffness, cracking strength, stiffness after cracking, load-deflection characteristics under cyclic loading, ultimate strength, mode of failure, strain distribution of the reinforcement, etc., were investigated and compared with theoretical results.

INTRODUCTION

Recently, box type or cylinder type reinforced concrete construction is frequently used for reactors and other structures. These box or cylinder walls may or may not be designed positively as an aseismic unit, but in any case large seismic force will concentrate into this type of wall unit due to its high rigidity. Hence the behavior of these wall units including restoring force characteristics, stress distribution, mode of failure and so on, should be investigated as a basic study not only for conventional aseismic design but also for dynamic design of structures involving such types of structural units. This paper reports an experimental study using small size reinforced concrete specimens.

This study was supported by the Japan Building Center and the Tokyo Electric Power Company.

OUTLINE OF TESTS

The experimental study was conducted at the University of Tokyo during April 1974 and May 1975. Seven specimens were made and subjected to static cyclic loading. Five specimens were square box type, 80cm high and 83 cm wide with 8cm wall thickness. Two were cylinder type, 80cm high and 85cm external diameter with 10cm wall thickness. They are shown in Fig.1.

Gross reinforcement ratios of box type specimens were 0.6%, 1.0% and 1.6%, vertically and horizontally. They were marked as B-6, B-10 and B-16 respectively. A specimen similar to B-10 had additional reinforcement in four corners to make the flexural capacity equal to B-16 and was marked as B-10R. Another specimen similar to B-10 was loaded diagonally, and was called B-10D. Gross reinforcement ratios of cylinder type specimens were 1.6% and 3.0%. They were marked as C-16 and C-30 respectively.

I Professor, Faculty of Engineering, University of Tokyo
II Associate Professor, Faculty of Engineering, University of Tokyo
III Formerly Research Assistant, Faculty of Engineering, University of Tokyo
IV Research Assistant, Faculty of Engineering, University of Tokyo

Average concrete properies for each specimen are summarized in Table 1. Yeild stress ${}_s\sigma_y$ of deformed bars (6, 10, 13 mm) was about 3900 kg/cm^2.

Specimens were placed in a steel loading frame, and clamped at the base by PC bars. Vertical loads were not applied. Cyclic horizontal loads were applied at the level of inner slab as shown in Fig. 1 by hydraulic jacks.

Table 1 shows bending and shear cracking load, ultimate load and the observed mode of failure. Fig. 2 shows skeleton curves of load-deflection relation for all seven specimens. It can be seen in Fig. 2 that all specimens showed "yield" point at the deflection angle between 1/200 and 1/100. Restoring force characteristics were quite similar for all specimens under cyclic loading at the amplitude up to this "yield" point. However, the behavior was quite different after this "yield" point up to the ultimate stage between flexural and shear failure type.

Crack patterns of B-10 and C-16 at the ultimate load are shown in Fig. 3. These specimens were flexural failure type, but many shear cracks were observed. Crack patterns of specimens failing in shear were similar to these except that definite shear failure took place at the end.

STRENGTH AND MODE OF FAILURE

Experimental results for cracking and strength are summarized in Table 1 together with theoretical results of the ultimate capacity for each specimen. The first bending crack appeared at the base of specimen and the first shear crack was found at the place ① shown in the indented figure of Table 1. The stress τ_c corresponding to the first shear crack in Table 1 was calculated based on the gross area ($\tau_c = Q_c/Ag$), and was found to be independent of the shear reinforcement ratio.

The flexural capacity was calculated by the approximate equation of full plastic theory shown in Fig. 4. This value coincided very well with the exact solution by the e-function theory[1)] for RC plasticity, applied to box type. For specimens B-6, B-10, B-10D and C-16, which were flexural failure type, flexural capacities calculated by the approximate method coincided well with the ultimate load in the experiments. Specimens B-16, B-10R and C-30, which were shear failure type, did not reach the calculated flexural capacity although it was observed in the test some flexural reinforcement yielded. The shear capacity was calculated as follows. First, ultimate shear stress was calculated by the Arakawa's equation[2)], which is usually used for beams. Then the web area was assumed as shown in Fig. 5 using neutral axis obtained from the calculation of flexural capacity. Shear capacity sQu was obtained as their product. Comparing calculated and measured values of specimens which failed in shear, the latter was found to be 30∿40 percent greater than the former.

On the other hand, for specimens which failed in bending, calculated shear capacity was reached in the tests. Calculated shear capacity for these specimens was higher than the calculated flexural capacity. It appeared that calculated shear capacity was generally too low, presumably because the restriction effect of flanges and slab to the web plate was neglected.

Failure mode, as determined by the smaller of the two calculated values, coincided with the observed mode. Although there involves some problem in the evaluation of shear capacity, the method as described above may be used to predict the mode of failure of structures such as box or cylinder types.

CONTRIBUTION OF WEB REINFORCEMENT

In order to examine the effect of web reinforcement, shear stress vs. strain relationships of reinforcement and concrete were obtained as follows.

(1) The flexural deflection δ_B determined from the measured axial deformation of flanges was subtracted from the total deflection δ_T to obtain shear deflection δ_S and average shear strain $\gamma = \delta_S/h$.

(2) The average shear stress in the web τ_ω was determined using the web area shown in Fig. 5.

(3) The average stress in the web reinforcement σ_t was obtained from the measured strains. From this average stress, the shear stress carried by web reinforcement τ_s was determined by the truss theory.

(4) The shear stress carried by concrete τ_c was determined by subtracting τ_s from τ_ω.

The relations between τ_ω, τ_c, τ_s and γ are shown in Fig. 6. Before the first shear crack was formed at ①, initial rigidity was nearly equal to the shear rigidity of concrete and the reinforcement carried no shear stress. After this crack appeared the shear stress in the reinforcement τ_s increased almost linearly. The greater the reinforcement ratio, the more effective the reinforcement was in carrying the shear. On the other hand, shear stress in the concrete, τ_c, became almost constant when cracks were formed at ② and ③. The value of this shear stress was about 0.1 Fc. Hence the total shear rigidity at this stage was strongly influenced by the reinforcement ratio.

INITIAL STIFFNESS

The observed initial stiffness shown in Fig. 7 was much smaller than the calculated values K_t, obtained by considering bending and shear deformation and assuming that all section is effective. It seemed that one of the causes would be that total width of the flange was not effective in case of box section. The effective width obtained from the flange stress distribution calculated by the elastic finite element method was 59 percent of the total flange width. The initial stiffness K_e using this effective width was reduced to about 80 percent of the initial stiffness K_t.

As it was conceivable that the cracks had been formed due to the shrinkage stress in the concrete before the loading or at the extremely initial stage, the stiffness was calculated assuming that the concrete on the tension side of the neutral axis was not effective. Both total and effective flange widths were used, and the resulted stiffness, crK_t and crK_e, respectively, were shown in Fig. 7.

It can be seen that the decline of the stiffness occurred before the cracks were found. As the stiffness after the break point almost coincided with $_{cr}K_e$, it was concluded that the cracks should have occurred at this point.

CONCLUSION

Five box type and two cylinder type reinforced concrete shear walls were subjected to cyclic loading to study the aseismic characteristics. According to the results presented herein, the following conclusions can be made:

(1) The first shear cracking stress τ_c was independent of the shear reinforcement ratio and τ_c = 0.03 Fc ∿ 0.05 Fc based on the gross area.

(2) Load-deflection curves up to the flexural yielding were similar irrespective of failure mode, but after that there was a difference of ductility between flexural and shear failure type. Deflection angle R at the maximum capacity was greater than 0.02 in case of flexural failure and about 0.015 in case of shear failure.

(3) The mode of failure could be determined by the smaller of the calculated capacities in flexure and shear.

(4) Before shear cracks were formed, entire shear stress was carried by concrete. After cracking, shear stress in concrete became constant and web reinforcement carried the increase of shear stress.

(5) The initial stiffness can be obtained by considering the effective width and neglecting the concrete on the tension side.

REFERENCES

1. H. Umemura, "Plastic Deformation and Ultimate Strength of Reinforced Concrete Beams," Transactions of the Architectural Institute of Japan No.42, Feb. 1951, pp.59-70.

2. T. Arakawa, "Allowable Unit Shearing Stress and Design Method of Shear Reinforcement of Reinforced Concrete Beams, Analyses of Existing Test Data," Concrete Journal, Japan Nat. Council on Concrete, Vol.8, No.7, July 1970, pp. 11-20.

3. H. Umemura, H. Aoyama, M. Itoh and Y. Hosokawa, "Experimental Study on the Restoring Force Characteristics of Reinforced Concrete Shear Walls, Part 1, 2 and 3," Proc. Kanto Dist. Symp., A.I.J., No.47, July 1976.

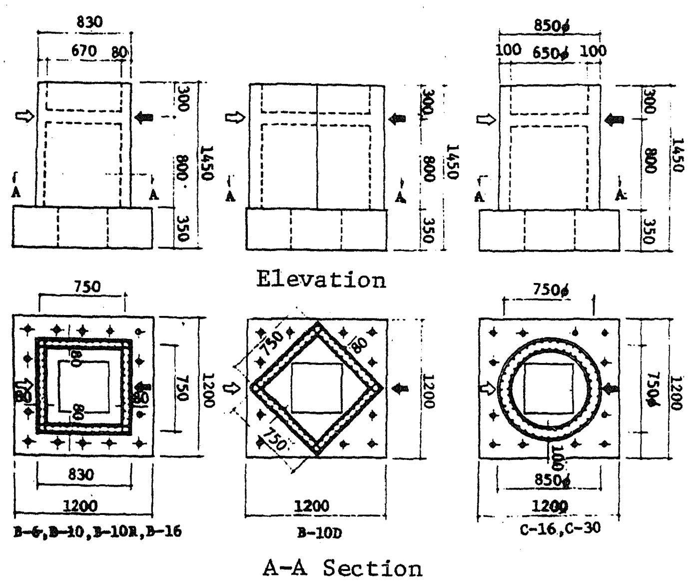

Fig. 1 Specimens Name & Dimension (mm)

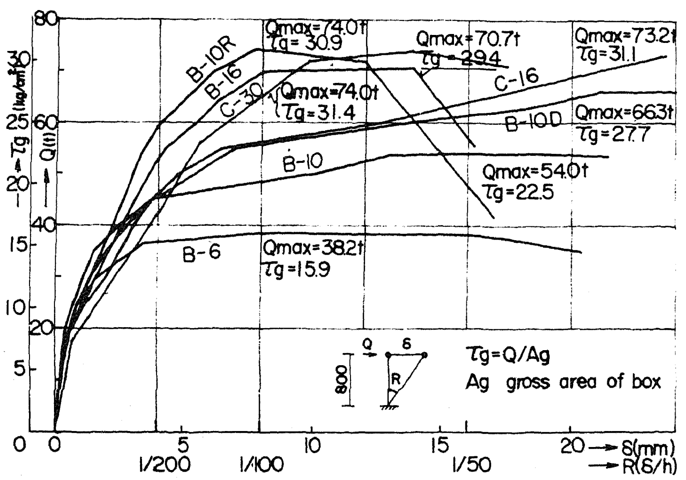

Fig. 2 Load-Delection Curves

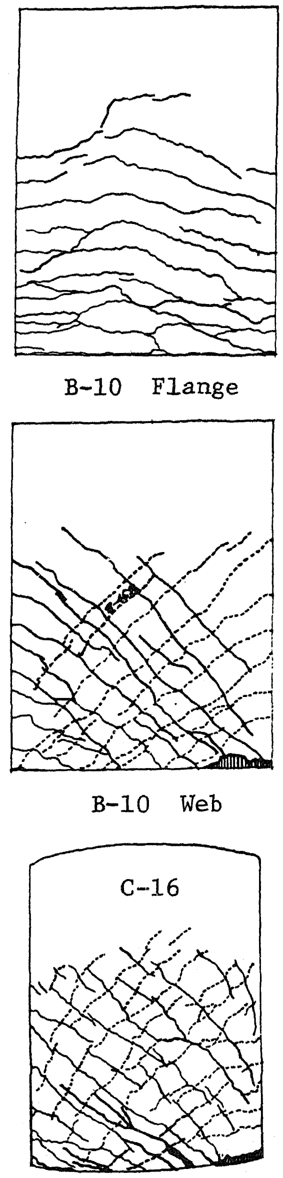

Fig. 3 Crack Pattern

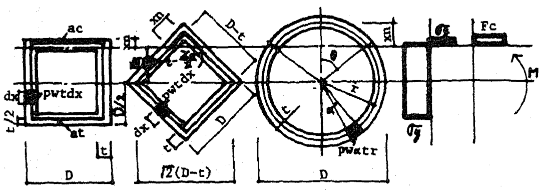

Fig. 4 Neutral Axis for Calculated Value of Bending Ultimate Strength

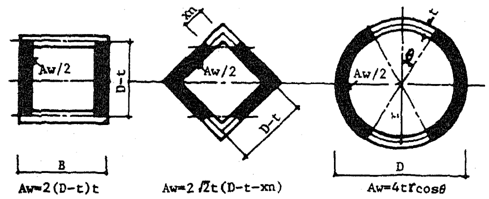

Fig. 5 Web Area for Calculated Value of Shear Strength

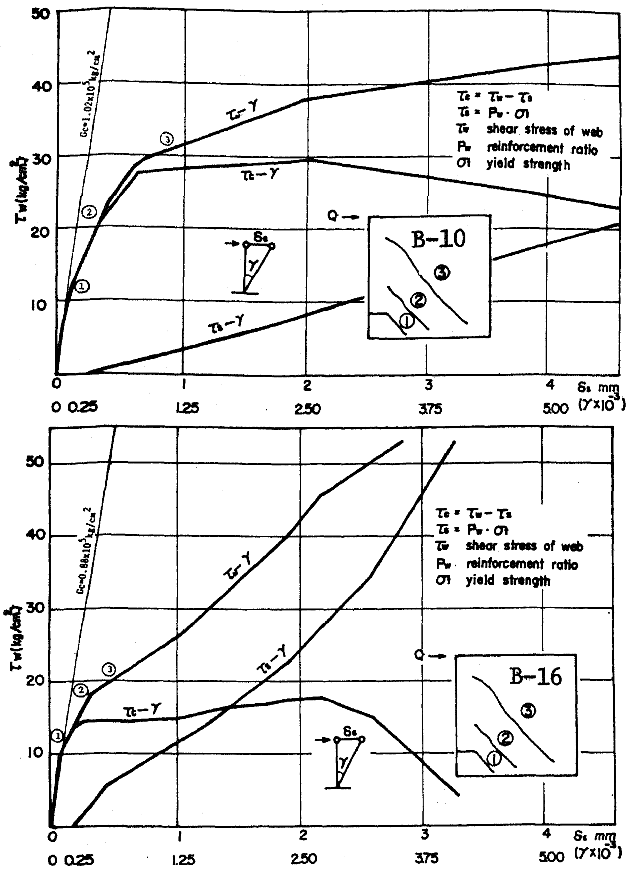

Fig. 6 Shear Stress in Web Reinforcement and Concrete

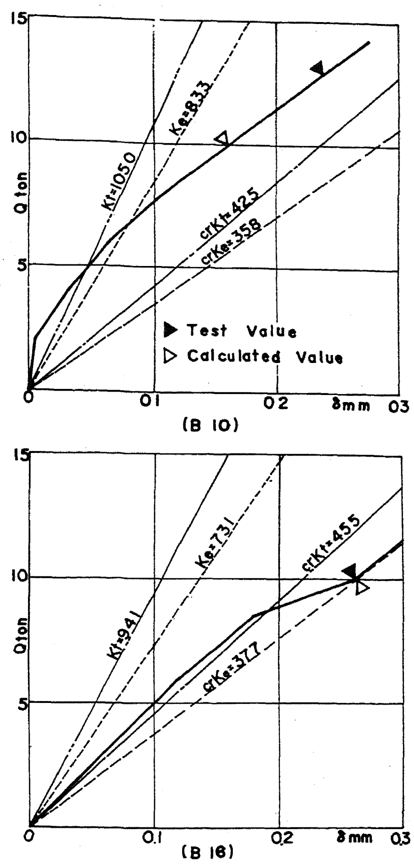

Fig. 7 Initial Stiffness

Table 1 Test Results and Failure Mode

Name of Specimen	Fc (kg/cm²)	Bending crack Test values: Mc (t·m)	Mc/Ze (kg/cm²)	shear crack Test values: Qc (t)	τ_c (kg/cm²)	τ_c/Fc	ultimate strength Test values: Qu (t)	τ_u (kg/cm²)	τ_u/Fc	Calculated values: sQu (t)	sQu (t)	T.V / C.V: Qu/sQu	Qu/sQu	Qu/Qc	Failure Mode
B- 6	256	8.0	14.5	20.0	8.3	0.032	38.2	15.9	0.062	44.5	34.3	0.85	1.11	1.82	Bending
B- 10	258	8.0	14.5	24.0	10.0	0.039	54.0	22.5	0.087	52.1	50.1	1.04	1.08	2.25	Bending
B- 16	190	8.0	14.5	15.0	6.3	0.033	70.0	29.4	0.154	55.1	75.1	1.27	0.93	4.71	Shear
B-10R	231	11.2	20.4	18.0	7.5	0.032	74.0	30.9	0.134	51.2	78.0	1.45	0.95	4.11	Shear
B-10D	268	11.2	30.4	24.0	10.0	0.037	66.3	27.7	0.103	61.2	58.7	1.08	1.11	2.76	Bending
C- 16	286	12.0	28.0	20.0	8.5	0.030	73.2	31.1	0.109	69.8	69.3	1.05	1.06	3.66	Bending
C- 30	175	–	–	19.8	8.4	0.048	74.0	31.4	0.179	52.6	113.9	1.41	0.65	3.74	Shear

Fc: compressive strength of concrete
Mc: cracking moment
Ze: section modulus (incl. bars)
$\tau_c(\tau_u) = \frac{Qc(Qu)}{Ag}$, Ag: gross area of section
Qc: shear at cracking type 1 as illustrated
Qu: ultimate shear
sQu: shear strength by Arakawa's eq.
sQu: bending strength by approximate eq.